Drug Design, Development and Therapy

Dovepress

open access to scientific and medical research

Open Access Full Text Article

ORIGINAL RESEARCH

Huangqi-Danshen Decoction Against Renal Fibrosis in UUO Mice via TGF-β1 Induced Downstream Signaling Pathway

Xi Huang[1,2,*], Yu Peng[1,2,*], Lingfei Lu[1,*], Liwen Gao[1,2], Shanshan Wu[1,2], Jiandong Lu[1], Xinhui Liu[1]

[1]Department of Nephrology, Shenzhen Traditional Chinese Medicine Hospital, Guangzhou University of Chinese Medicine, Shenzhen, Guangdong, People's Republic of China; [2]The Fourth Clinical Medical College, Guangzhou University of Chinese Medicine, Shenzhen, Guangdong, People's Republic of China

*These authors contributed equally to this work

Correspondence: Xinhui Liu, Department of Nephrology, Shenzhen Traditional Chinese Medicine Hospital, Guangzhou University of Chinese Medicine, Shenzhen, Guangdong, 518033, People's Republic of China, Email liuxinhui0317@163.com

Background: Huangqi-Danshen decoction (HDD) is a Chinese medicinal herb pair with good efficacy in treating chronic kidney disease, but its mechanism needs to be clarified.

Aim: To uncover the underlying mechanism of HDD antagonizing renal fibrosis through network pharmacology (NP) analysis and experimental validation.

Materials and Methods: The chemical components of water extract of HDD were analyzed by combining the ultra-high performance liquid chromatography coupled with Q-Exactive mass spectrum analysis (UHPLC-QE-MS) and HERB database. NP was used to identify core common targets of HDD components and renal fibrosis. Subsequently, male C57BL/6 mice were divided into Sham, unilateral ureteral obstruction (UUO) and UUO+HDD groups. Renal function, histopathology, Western blotting, and immunohistochemistry analyses were used to evaluate the protective effect of HDD on UUO mice. The effects of HDD on signaling pathways were validated in both UUO mice and transforming growth factor-β1 (TGF-β1)-induced HK-2 cells.

Results: By combining UHPLC-QE-MS analysis and HERB database, 25 components were screened in HDD extract. There were 270 intersection targets of the 25 components and renal fibrosis. Based on their scores in protein-protein interaction analysis and degree values in component-pathway-target triadic network, 6 core common targets of the 25 components and renal fibrosis were identified, namely phosphoinositide 3-kinase (PI3K), signal transducer and activator of transcription 3 (Stat3), non-receptor tyrosine kinase Src (Src), epidermal growth factor receptor (EGFR), matrix metalloproteinase 9 (MMP9), and MMP2. HDD ameliorated renal tubular damage and collagen deposition and downregulated fibrosis-related proteins expression in UUO mice. Furthermore, HDD was demonstrated to reduce PI3K, Stat3, Src, EGFR, and MMP2 expressions, and enhance MMP9 expression in the kidney of UUO mice and in TGF-β1-induced HK-2 cells.

Conclusion: HDD can alleviate renal fibrosis which may be related to regulating the expression of essential proteins in the epithelial-mesenchymal transition and extracellular matrix production/degradation signaling pathways.

Keywords: renal fibrosis, chronic kidney disease, Huangqi-Danshen decoction, network pharmacology, signaling pathway

Introduction

By 2040, chronic kidney disease (CKD), which is becoming more prevalent, will rank as the fifth greatest cause of premature death globally.[1,2] According to current international guidelines, CKD is defined as a deterioration in renal function, or markers of renal damage, that lasts for a minimum of 3 months, regardless of the underlying etiology.[3] CKD, which can proceed to end-stage renal disease or early mortality from cardiovascular problems, is frequently brought on by hypertension and diabetes.[3] CKD has gained attention as an important health issue in recent years, requiring significant financial and social resources.[1] However, the etiology and pathogenesis of CKD are still under investigation.

Received: 9 February 2024
Accepted: 10 September 2024
Published: 14 September 2024

Graphical Abstract

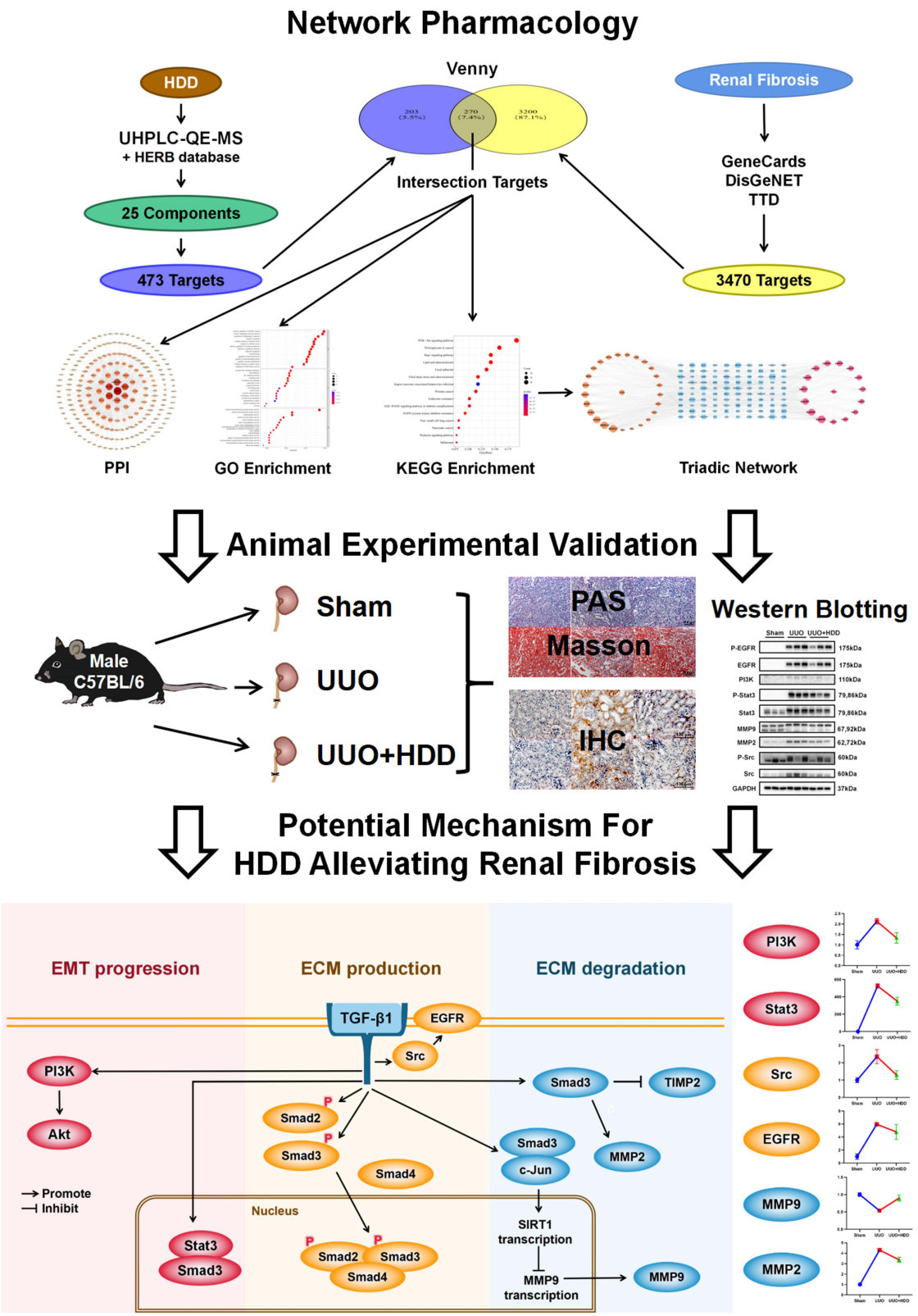

It is believed that renal fibrosis is an essential marker of CKD, and its degree is closely related to CKD stage and clinical prognosis.[4] Extracellular matrix (ECM) contributes to renal fibrosis by increasing production and deposition, destroying normal kidney structure.[5] The primary factor accelerating CKD progression is renal fibrosis. Treatment of CKD must therefore target the alleviation of renal fibrosis.

With the limited treatment of current mainstream, in both the avoiding and remedying of CKD, traditional Chinese medicine (TCM) has an extensive background and a considerable impact. Based on the clinical characteristics of CKD patients, Qi deficiency and blood stasis is the main type of TCM syndrome. Hence, Qi invigoration and blood activation are the key strategies in TCM for preventing and treating CKD. Huangqi-danshen decoction (HDD), which comprises the herbs Huangqi (Astragali Radix) and Danshen (Salviae Miltiorrhizae Radix et Rhizoma), is utilized in the healing process of CKD in clinical settings for invigorating Qi and activating blood.[6–8] Both Huangqi and Danshen were originally mentioned in the Shennong's Classic of Materia Medica (Shennong Bencao Jing, pinyin in Chinese) in the Eastern Han Dynasty (AD 25–220).[9] In TCM practice, Huangqi is used to tonify Qi and Danshen is used to promote blood circulation. According to TCM treatment principles, Huangqi and Danshen are usually prescribed for patients with CKD.[6] Our earlier studies have revealed the benefits of HDD in reducing renal fibrosis and delaying CKD progression.[10–13] The fundamental mechanisms, however, have yet to be clarified.

There is a paradigm of treatment in TCM known as "multi-target, multi-component",[14] that breaks the shackles of organ-centric medicine and the one-target, one-drug dogma.[15] By using network pharmacology (NP), herbals can be detected chemically, potential active ingredients screened, and targets predicted for related illnesses explored.[16] In our current investigation, we firstly screened the components in HDD extract by combining the ultra-high performance liquid chromatography coupled with Q-Exactive mass spectrum (UHPLC-QE-MS) analysis and HERB database. Then, we used NP to identify the core common targets of the screened components and renal fibrosis. Subsequently, unilateral ureteral obstruction (UUO) mice model and transforming growth factor-β1 (TGF-β1)-induced HK-2 cells were applied to validate the antifibrotic response of HDD and its regulation on the identified targets.

Materials and Methods

Components Screening

HDD Extract

There are two components of HDD: Huangqi (Astragali Radix [*Astragalus membranaceus (Fisch). Bge.var. mongholicus (Bge). Hsiao*]) and Danshen (Salviae Miltiorrhizae Radix et Rhizoma [*Salvia miltiorrhiza Bunge*]). Raw herbs of Huangqi and Danshen were purchased from Shenzhen Huahui Pharmaceutical Co., Ltd. (Shenzhen, China). HDD extract was prepared in our laboratory according to the following procedure. After soaking Huangqi and Danshen in 10 times (*w/v*) of double-distilled water (ddH_2O) for 30 min, the herbs were boiled for 1 hour for extraction. The extracted solution was collected, and the herbs were then heated for an additional hour with 8 times (*w/v*) as much ddH_2O. A final concentration of 1 g of raw herb per mL was achieved by combining, filtering, and concentrating the extracts that were obtained twice.

UHPLC-QE-MS Analysis

The samples were centrifuged at 12,000 rpm for 15 min at 4 °C after being defrosted on ice for 30s. After adding 1000 mL of extract (methanol: water = 4:1, IS = 1000: 10) to 300 mL of supernatant in an EP tube, samples were sonicated in an ice water bath for 5 min, and then incubated at −40 °C for 1 h before being centrifuged at 12,000 rpm for 15 min at 4 °C. The supernatant was injected into the sample container and passed through a 0.22 μm filter membrane before being blended with 200 μL of each sample for machine detection.

A Waters UPLC BEH C18 column (1.7 μm 2.1×100 mm) was used for the LC-MS/MS study on an Agilent ultra-high performance liquid chromatography 1290 UPLC system. A flow rate of 400 μL/min was applied, and a sample injection volume of 5 μL was used. Both 0.1% formic acid in water (A) and 0.1% formic acid in acetonitrile (B) consisted of the mobile phase. Elution follows a gradient linear procedure. Based on the IDA acquisition mode, the MS and MS/MS data were obtained using a Q Exactive Focus mass spectrometer and the Xcalibur software. The mass range for each acquisition cycle was 100 to 1500, and the top three results from each cycle were filtered before the matching MS/MS

data were further obtained. XCMS software was used to import raw mass spectrometry data.[17] After retention time correction, peaks with MS/MS data were identified. The components in HDD extract were screened by combining the results of UHPLC-QE-MS analysis and HERB database (http://herb.ac.cn/).[18]

Network Pharmacology Analysis

Prediction of Targets of the Screened Components in HDD

The screened components in HDD were entered into PubChem (https://pubchem.ncbi.nlm.nih.gov/) and converted into canonical SMILES format. Next, the canonical SMILES format files were imported into the SwissTargetPrediction platform (http://www.swisstargetprediction.ch/), and the attribute was set to "Homo Sapiens" to obtain the predicted targets of these components. The known targets of these components were supplemented according to literature reports. Then, the UniProt database (https://www.uniprot.org/) was used to normalize and standardize these targets, and finally the targets of components were obtained after duplication was deleted.

Targets Screening of Renal Fibrosis

The GeneCards database (https://www.genecards.org/), DisGeNET database (https://www.disgenet.org), and TTD database (http://db.idrblab.net/ttd/) were used to search for potential targets of renal fibrosis. In GeneCards database, the higher the Relevance score, the closer the target is to disease. If there were too many targets, set the target with a Relevance score greater than the median as the potential target of renal fibrosis. After merging the three disease database targets, the renal fibrosis targets were obtained by deleting duplicates. The gene names of the targets were corrected using the UniProt database (https://www.uniprot.org/).

Constructing the Protein-Protein Interaction Network

Drawing a Venn diagram of HDD components targets and renal fibrosis targets in Venny 2.1 (https://bioinfogp.cnb.csic.es/tools/venny/index.html) to find crossover targets. The protein-protein interaction (PPI) network model of intersection targets was constructed by STRING11.5 (https://string-db.org). Set the biological species to "Homo sapiens", set the minimum interaction threshold to "highest confidence (> 0.9)", and hide disconnected nodes in the network. The other settings were all default settings. Visualization and analysis of PPI network were implemented by Cytoscape 3.9.0 software (National Resource for Network Biology, USA). The Cytoscape 3.9.0 plug-in analyze network was applied to calculate the topological parameters of individual nodes in the network. In this network diagram, nodes were used to represent components and targets, and edges were used to represent node interactions.

Gene Enrichment Analysis and Component-Pathway Network Building

The threshold was set at $P < 0.05$ for the gene ontology (GO) and Kyoto encyclopedia of genes and genomes (KEGG) enrichment analysis performed using the clusterprofiler package in R studio software (https://www.rstudio.com/). The enrichment results were visualized by ggplot2 package. The top 15 pathways of biological process (BP), cellular component (CC), and molecular function (MF) modules were selected to draw GO bubble diagram. The top 15 pathways in KEGG were plotted as bubble and chord diagrams. HDD component-renal fibrosis intersection targets and the targets included in the top 15 signaling pathways of KEGG were introduced into Cytoscape 3.9.0 software to obtain the HDD component-renal fibrosis-pathway network diagram.

Animals

A total of 18 male C57BL/6 mice, aged 6 weeks and weighing 20 ± 2 g, were purchased from Guangdong Medical Laboratory Animal Center (Foshan, China). Three groups of mice were divided randomly after seven days of adaptation: Sham (n = 6), UUO (n = 6), and UUO+HDD (n = 6). Mice in the UUO and UUO+HDD groups were subjected to UUO to induce renal fibrosis. In accordance with established protocols, the UUO surgery was carried out by ligating the left ureter with surgical silk.[19] Sham mice were only subjected to bluntly separated without ligation of the ureter. HDD extract (6.8 g/kg/day) was administered to mice in the UUO+HDD group 3 days prior to the modeling procedure by gastric irrigation. All mice were killed on day 7 after UUO surgery. Tissue samples from the UUO ipsilateral kidney and blood samples acquired by ocular enucleation were collected for follow-up analysis. All animal experiments were

complied with the ARRIVE guidelines and were carried out in accordance with the UK Animals (Scientific Procedures) Act, 1986 and associated guidelines. Due to the limitations of our hospital's animal experimentation facilities and long waiting time for appointments, we chose Shenzhen TopBiotech Co., Ltd to conduct the animal experiments and obtained approval from the Ethics Committee (approved ID: TOP-IACUC-2022-0203).

Renal Function and Pathology Analysis

Serum creatinine (Scr) and blood urea nitrogen (BUN) were assayed with the corresponding detection kits (#SKT-217 and # SKT-213, StressMarq Biosciences, British Columbia, Canada). Dehydrated and paraffin embedded kidney samples were fixed in 4% paraformaldehyde overnight at 4 °C. Periodic acid-Schiff stains (PAS) and Masson's trichrome stains were used on the 4-mm kidney sections. PAS staining was used to quantify tubular dilatation, atrophy, and vacuolation based on a modified six-point scoring system (grades 0–5): grade 0 (no injury), grade 1 (≤ 10%), grade 2 (10 – 25%), grade 3 (25 – 50%), grade 4 (50 – 75%), and grade 5 (≥ 75%).[20] ImageJ (NIH, Bethesda, MD, USA) was used to measure the collagen-occupied areas in Masson staining. The collagen volume fraction (%) was then calculated by dividing those areas by the entire area under examination. All scoring procedures were carried out under blind conditions.

Immunohistochemistry

Slices of 6 μm thick were made from the kidney tissues, which were then embedded in paraffin and preserved with 4% paraformaldehyde. Kidney sections were reacted with antigen retrieval, goat serum blocking, and overnight incubations at 4 °C with α-SMA, TGF-β1, PI3K, P-Stat3, MMP9, and P-Src. After reacted with secondary antibodies, the positive areas were observed with DAB enzyme-linked anti-mouse/rabbit IgG polymer reagent under close observation with microscope for 30s-10min. All sections were covered in hematoxylin for 5 min and differentiated with acidic ethanol differentiation solution (1%) for 1–3s and restored the elution before sealing. ImageJ software (National Institutes of Health, Bethesda, MD, USA) was used to compute the integrated optical density.

Cell Culture and Treatment

The renal proximal tubular epithelial cell line (HK-2) was purchased from Pricella Biotechnology Co., Ltd. (Wuhan, China). HK-2 cells were cultured in DMEM/F12 medium containing 10% fetal bovine serum, 100 U/mL penicillin, and 100 μg/mL streptomycin (Thermo Fisher Scientific, Waltham, MA, USA). Cell culture was maintained in a humidified atmosphere at 37°C with 5% CO_2. After reaching 80% confluence, HK-2 cells were treated with 10 ng/mL TGF-β1 (PeproTech, Rocky Hill, NJ, USA) in the absence or presence of HDD (5 mg/mL) for 48 h. For mechanism, HK-2 cells were pretreated with EGFR agonist NSC228155 (0.625 μM) or Stat3 agonist colivelin (1 μM) for 2 h, followed by treatment with TGF-β1 or combined HDD for an additional 48 h.

Western Blot Analysis

Kidney tissues or cells from different groups were dissolved in RIPA buffer [#9806, Cell Signaling Technology (CST)] supplemented with protease inhibitor cocktail (04693124001, Roche) and phosphatase inhibitor cocktail (04906837001, Roche). The kidney lysates were electrophoresed in 7–10% SDS-PAGE gels, and then transmembrane with 0.45 μm polyvinylidene difluoride membranes were used. The membranes were reacted with primary antibodies against fibronectin (FN, ab2413, Abcam), α-smooth muscle actin (α-SMA, A5228, Sigma-Aldrich), transforming growth factor-β1 (TGF-β1, ab179695, Abcam), Phospho-Smad2/3 (P-Smad2/3, #8828, CST), Smad2/3 (#8685, CST), phosphoinositide 3-kinase (PI3K, #4249, CST), Phospho- signal transducer and activator of transcription 3 (P-Stat3, #9145, CST), Stat3 (#9139, CST), Phospho-Src (P-Src, #2101, CST), Src (#2109, CST), Phospho-epidermal growth factor receptor (P-EGFR, #3777S, CST), EGFR (#4267S, CST), matrix metalloproteinase-9 (MMP9, 10375-2-AP, Proteintech), matrix metalloproteinase-2 (MMP2, 10373-2-AP, Proteintech), and glyceraldehyde-3-phosphate dehydrogenase (GAPDH, 60004-1-1g, Proteintech) at 4 °C overnight. The secondary antibodies were then applied to the membranes and incubated. Membranes were imaged and quantitated using Image Lab software 5.1 (Bio-Rad Laboratories, Hercules, CA, USA).

Statistical Analysis

Data were expressed as the mean ± standard error of mean (SEM). For normally distributed data, One-way ANOVA followed by Dunnett multiple comparisons test was used for comparison between groups. For non-normally distributed data, the Kruskal–Wallis test followed by Dunn's multiple comparisons test was used for comparison between groups. All analyses were conducted using GraphPad Prism 9.0 (La Jolla, CA, USA). A P value < 0.05 was considered statistically significant.

Results

Component Analysis of HDD and Targets Prediction

By combining UHPLC-QE-MS analysis and HERB database, 25 components were screened in HDD extract (Table 1 and Figure 1). Vanillic acid, sucrose, ononin, daidzein, dihydrocapsaicin, astragaloside II, astragaloside III, astragaloside IV, and formononetin were derived from Astragali Radix. Isoimperatorin, ferulic acid, danshensu, caffeic acid, carnosol, rosmarinic acid, lithospermic acid, protocatechualdehyde, salvianolic acid A, salvianolic acid B, salvianolic acid C, ursolic acid, apigenin, cryptotanshinone, and tanshinone IIA were derived from Salviae Miltiorrhizae Radix et Rhizoma. Isoferulic acid was derived from both Astragali Radix and Salviae Miltiorrhizae Radix et Rhizoma (Table 1). By the SwissTargetPrediction platform, 473 targets of the 25 components were determined (Supplementary Table S1). A total of 3470 targets of renal fibrosis were obtained in GeneCards, DisGeNET, and TTD database (Supplementary Table S2). The Venn diagram yielded 270 intersection targets of HDD components and renal fibrosis (Figure 2A). In PPI network analysis, Src was the highest scoring target, followed by Stat3, phosphoinositide-3-kinase regulatory subunit 1 (PIK3R1), heat shock protein 90-alpha (HSP90AA1), and phosphatidylinositol-4,5-bisphosphate 3-kinase catalytic subunit alpha (PIK3CA) (Figure 2B). These results suggested that Src, Stat3, and PI3K were core common targets of HDD components and renal fibrosis.

Table 1 Details of the 25 Components in HDD Extract

Peak No.	ID.	Retention Time (min)	Adduct Ion	Theoretical Mass (m/z)	Experimental Mass (m/z)	Error (ppm)	Formula	Identification	Source
1	HDD1	2.69	$[M-H]^-$	269.082	269.0820	0.12	$C_{16}H_{14}O_4$	Isoimperatorin	SMRR
2	HDD2	2.97	$[M-H]^-$	167.035	167.0351	0.72	$C_8H_8O_4$	Vanillic acid	AR
3	HDD3	4.43	[M-H]	341.108	341.1093	0.90	$C_{12}H_{22}O_{11}$	Sucrose	AR
4	HDD4	5.08	[M+H]	195.065	195.0649	0.45	$C_{10}H_{10}O_4$	Ferulic acid	SMRR
5	HDD5	5.37	[M+H]	195.065	195.0649	0.54	$C_{10}H_{10}O_4$	Isoferulic acid	AR/SMRR
6	HDD6	5.99	[M-H]	197.045	197.0451	0.26	$C_9H_{10}O_5$	Danshensu	SMRR
7	HDD7	6.05	[M+H]	181.049	181.0492	1.20	$C_9H_8O_4$	Caffeic acid	SMRR
8	HDD8	6.06	[M+H]	331.191	331.1895	1.48	$C_{20}H_{26}O_4$	Carnosol	SMRR
9	HDD9	6.14	$[M+H-H_2O]^-$	343.083	343.0804	1.16	$C_{18}H_{16}O_8$	Rosmarinic acid	SMRR
10	HDD10	6.21	[M+H]	539.118	539.1185	0.88	$C_{27}H_{22}O_{12}$	Lithospermic acid	SMRR
11	HDD11	6.67	[M+H]	431.134	431.1332	0.37	$C_{22}H_{22}O_9$	Ononin	AR
12	HDD12	6.71	$[M+H]^+$	255.065	255.0644	1.47	$C_{15}H_{10}O_4$	Daidzein	AR
13	HDD13	6.82	[M+H]	139.039	139.0387	2.16	$C_7H_6O_3$	Protocatechualdehyde	SMRR
14	HDD14	7.63	[M+H]	308.223	308.2217	2.22	$C_{18}H_{29}NO_3$	Dihydrocapsaicin	AR
15	HDD15	7.76	[M+H]	493.113	493.1128	0.45	$C_{26}H_{20}O_{10}$	Salvianolic acid C	SMRR
16	HDD16	8.26	[M-H]	493.115	493.1146	1.25	$C_{26}H_{22}O_{10}$	Salvianolic acid A	SMRR
17	HDD17	8.31	[M+H]	785.468	785.4638	2.75	$C_{41}H_{68}O_{14}$	Astragaloside IV	AR
18	HDD18	8.82	[M-H]	267.066	267.0664	1.48	$C_{16}H_{12}O_4$	Formononetin	AR
19	HDD19	9.17	[M-H]	783.453	783.4529	1.45	$C_{41}H_{68}O_{14}$	Astragaloside III	AR
20	HDD20	9.78	[M+H]	827.478	827.4664	10.38	$C_{43}H_{70}O_{15}$	Astragaloside II	AR
21	HDD21	10.08	$[M+H-H_2O]^-$	439.36	439.3555	1.16	$C_{30}H_{48}O_3$	Ursolic acid	SMRR
22	HDD22	10.93	$[M-H]^-$	269.046	269.0454	1.40	$C_{15}H_{10}O_5$	Apigenin	SMRR
23	HDD23	13.06	[M+H]	297.148	297.1479	0.25	$C_{19}H_{20}O_3$	Cryptotanshinone	SMRR
24	HDD24	13.29	[M+H]	295.133	295.1319	0.45	$C_{19}H_{18}O_3$	Tanshinone IIA	SMRR
25	HDD25	6.94	$[M+NH_4]^+$	736.188	736.1846	0.61	$C_{36}H_{30}O_{16}$	Salvianolic acid B	SMRR

Abbreviations: AR, Astragali Radix; SMRR, Salviae Miltiorrhizae Radix et Rhizoma.

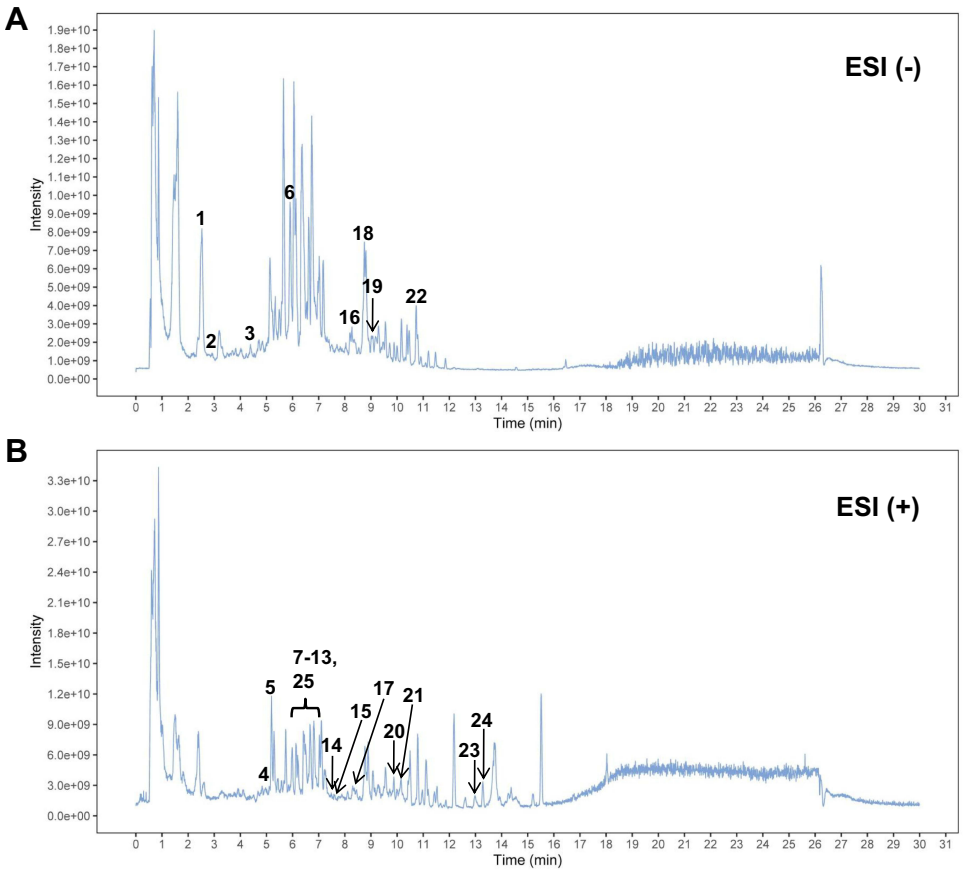

Figure 1 The total ion chromatograms (TICs) of HDD extract in the negative (**A**) and positive (**B**) ion modes. The numbers represent the 25 components identified.
Abbreviation: ESI, electron spray ionization.

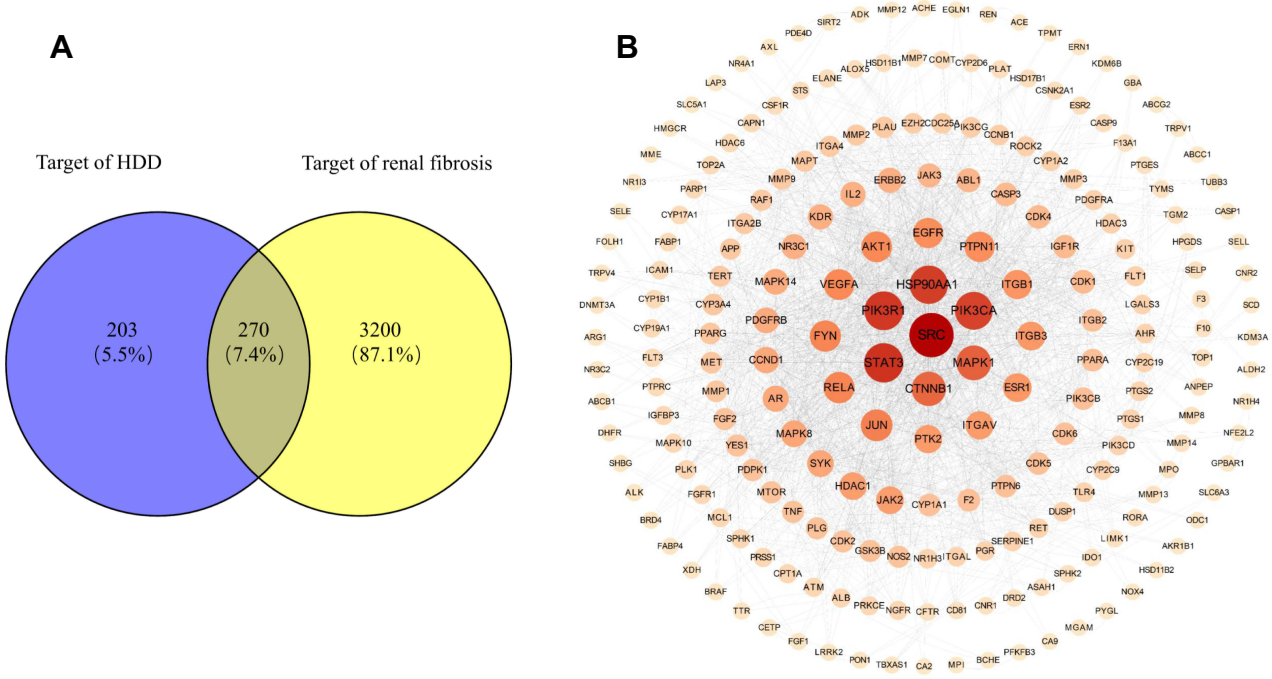

Figure 2 The interaction of shared targets between HDD components and renal fibrosis. (**A**) The Venn diagram. (**B**) PPI network of 270 intersection targets.

Enrichment Analysis and Component-Pathway-Target Triadic Network Construction

Taking $P < 0.05$ as the screening condition, a total of 3291 GO enrichment analysis results were obtained, including 2863 biological processes, 150 cell components, and 278 molecular functions. The top 15 results were shown in Figure 3A. $P < 0.05$ screening was performed on a total of 171 KEGG enrichment analysis results. The results showed 15 pathways ranked highly (Figure 3B). The visual results of network analysis of KEGG were shown in Figure 3C. These results showed that targets of HDD against renal fibrosis mainly enriched in energy metabolism, apoptosis, inflammation, and oxidative stress related pathways, containing PI3k/Akt signaling pathway, proteoglycans in cancer, rap1 signaling pathway, lipid and atherosclerosis, focal adhesion and so on. In component-pathway-target triadic network, the top 5 target proteins were screened out according to degree value, which were EGFR, MMP9, Stat3, MMP2, and PIK3CA (Figure 4). Combined with PPI results, 6 target proteins including PI3K, Stat3, Src, EGFR, MMP9, and MMP2 were finally identified for experimental verification.

HDD Improved Renal Pathological Injury in UUO Mice

Results of Scr and BUN did not markedly differ from those in the Sham group between the UUO group and the UUO +HDD group (Figure 5A and B), suggesting UUO may have little effect on renal function in mice in the short term (7-day). However, in contrast to Sham mice, UUO animals showed notable tubular injury in PAS staining, including tubular cell atrophy and degeneration as well as vacuolar lesions in kidney tissue (Figure 5C and D). Masson staining displayed obvious collagen deposition in renal tubular interstitium of UUO mice (Figure 5E and F). HDD treatment markedly reduced tubular injury and collagen volume fraction in UUO mice ($P < 0.001$, Figure 5C–F). These findings showed how effectively HDD may protect the renal structure in UUO mice.

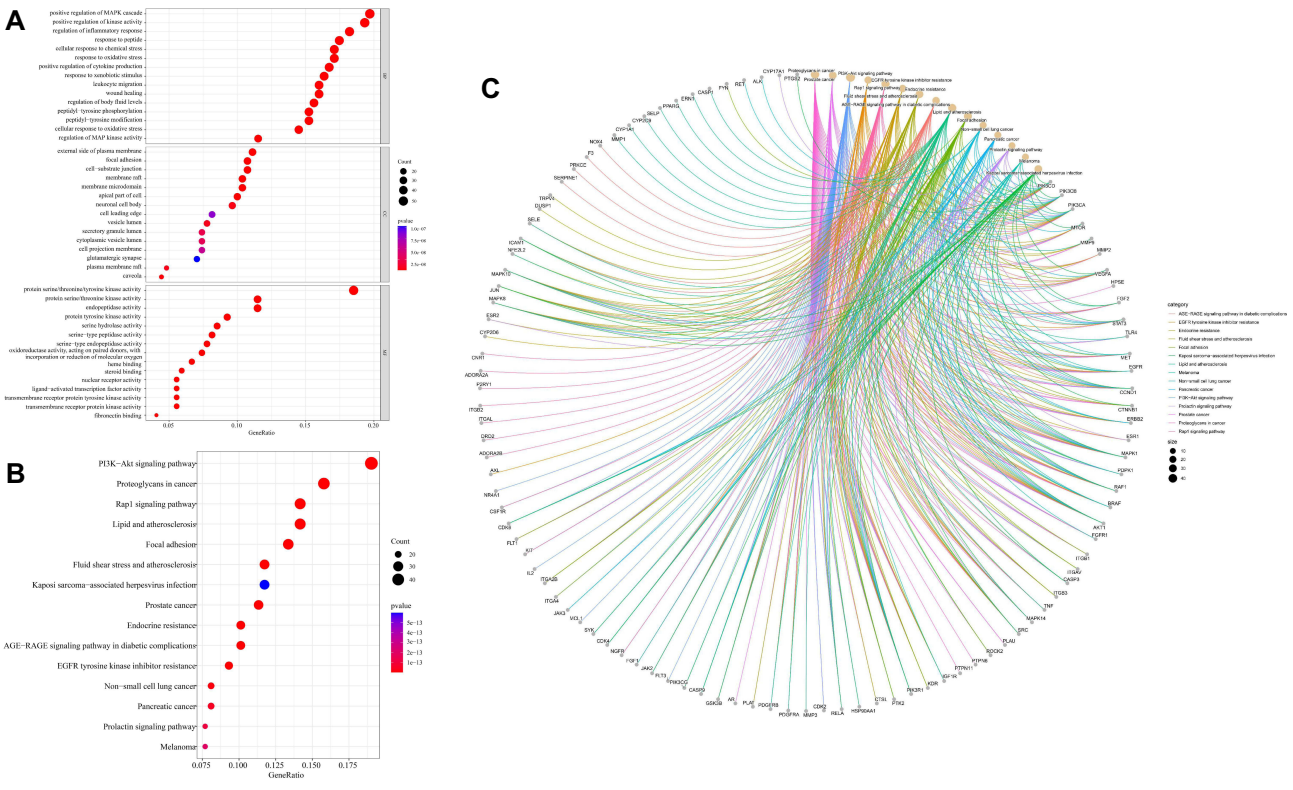

Figure 3 Gene enrichment analysis. (**A**) Bubble chart of the top 15 pathways for the GO enrichment analysis based on the common targets of HDD components and renal fibrosis. (**B**) Bubble chart of the top 15 pathways for the KEGG enrichment analysis from the common targets between HDD components and renal fibrosis. (**C**) Chord chart of KEGG enrichment analysis. The 15 yellow bubbles represent signaling pathways, and the grey bubbles represent targets.

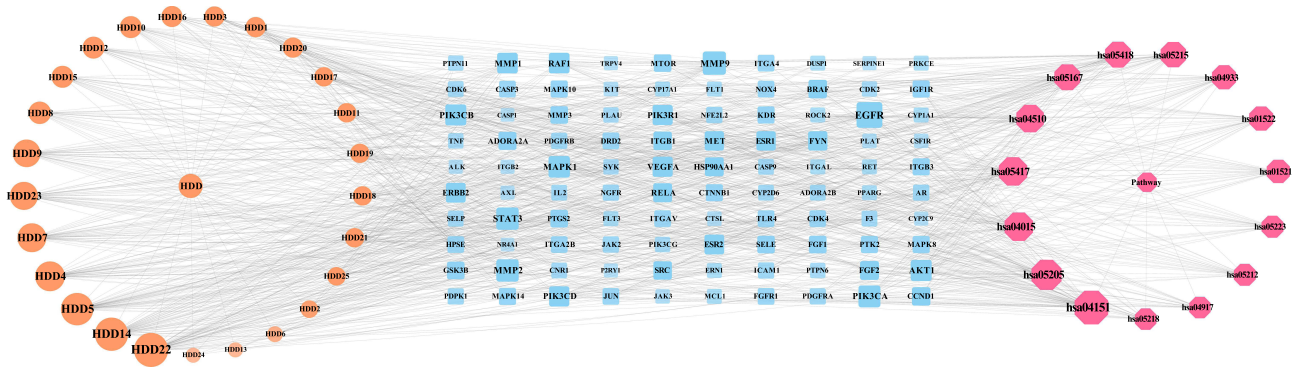

Figure 4 The component-pathway-target triadic network construction. The Orange circulars represent 25 HDD components. The blue rectangles represent targets of HDD components and renal fibrosis. The pink hexagons represent the top 15 signaling pathways.

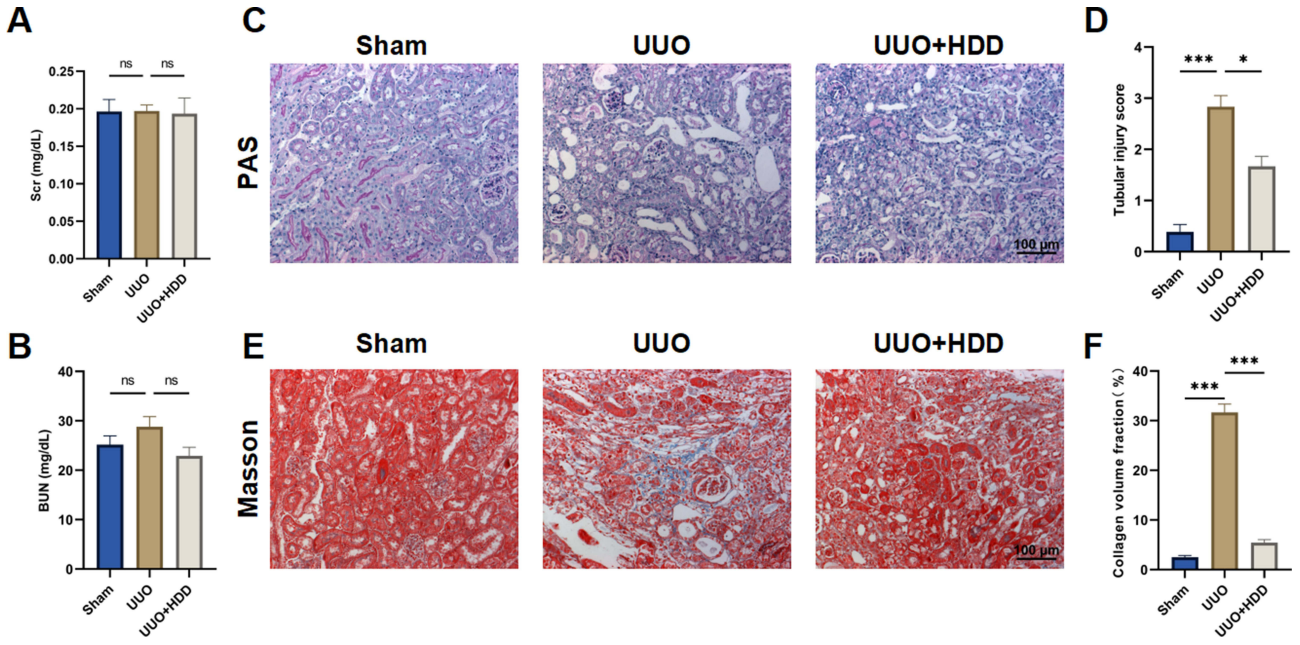

Figure 5 Effects of HDD on UUO mice. (**A**) Serum creatinine. (**B**) Blood urea nitrogen. (**C**) Representative PAS staining images. All images are shown at identical magnification, × 200, scale bar = 100 μm. (**D**) Tubular injury score. (**E**) Representative Masson staining images. All images are shown at identical magnification, × 200, scale bar = 100 μm. (**F**) Collagen volume fraction (%). Data are expressed as mean ± SEM, n = 6 mice per group, ns = no significance, *$P < 0.05$, ***$P < 0.001$.
Abbreviations: BUN, blood urea nitrogen; Scr, serum creatinine.

HDD Diminished Renal Fibrosis in UUO Mice

According to Western blotting, the expressions of FN, α-SMA, TGF-β1, and P-Smad2/3 were obviously enhanced in the kidney of UUO mice ($P < 0.001$). The above fibrosis indicators were greatly decreased in expression after HDD therapy ($P < 0.05$, Figure 6A and B). Further IHC validation showed UUO mice had higher expression of α-SMA and TGF-β1 compared with Sham mice ($P < 0.001$). Administration of HDD downregulated α-SMA and TGF-β1 compared with the UUO group ($P < 0.001$, Figure 6C and D). Both Western blot and IHC analyses proved that HDD alleviated renal fibrosis in UUO mice.

HDD Regulated the Expression of Fibrosis-Related Signals in the Kidney of UUO Mice and TGF-β1-Induced HK-2 Cells

In order to validate the results of NP, we analyzed the expression changes of PI3K, Stat3, Src, EGFR, MMP9, and MMP2 in different ways. In Western blotting, UUO elevated the expressions of PI3K ($P < 0.05$), Stat3 ($P < 0.001$), Src ($P < 0.05$), and EGFR ($P < 0.001$) in comparison to the Sham group. In contrast, the expression of MMP9 ($P < 0.001$) was diminished in the

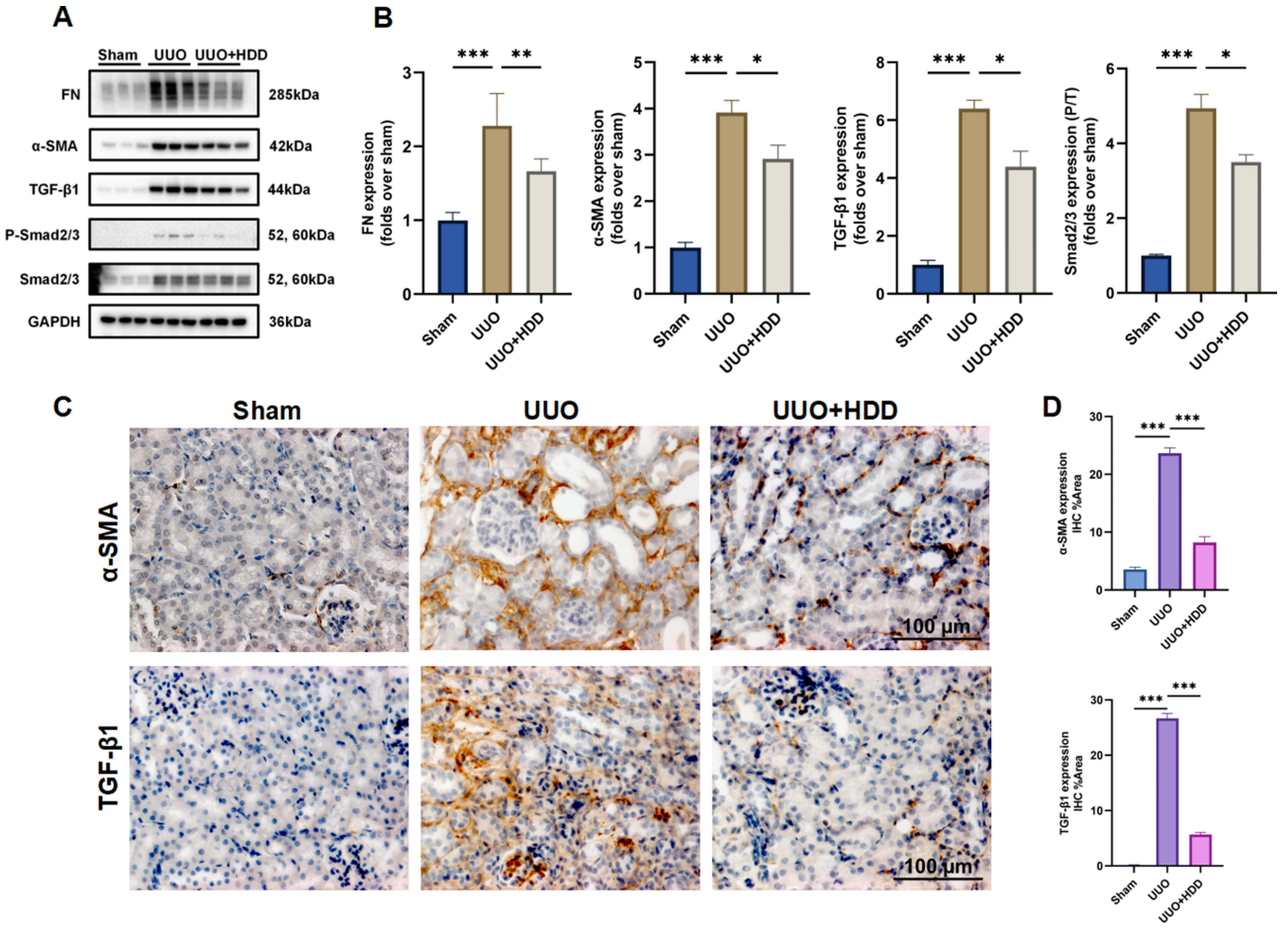

Figure 6 Effects of HDD on renal fibrosis in UUO mice. (**A**) Western blot images of FN, α-SMA, TGF-β1, P-Smad2/3, and Smad2/3 expression in the kidney. (**B**) Quantitative analysis of FN, α-SMA, TGF-β1, and Smad2/3 (phosphorylated/total) expression, folded over sham, normalized to GAPDH. Data are expressed as mean ± SEM, n = 6 mice per group, **P* < 0.05, ***P* < 0.01, ****P* < 0.001. (**C**) Representative IHC images of α-SMA and TGF-β1 in kidneys. All images are shown at identical magnification, × 400, scale bar = 100 μm. (**D**) Quantitative analysis of α-SMA and TGF-β1 expression in IHC. Data are expressed as mean ± SEM, n = 5 mice per group, ****P* < 0.001.
Abbreviations: α-SMA, α-smooth muscle antibody; FN, fibronectin; GAPDH, glyceraldehyde-3-phosphate dehydrogenase; P-Smad2/3, Phospho-Smad2/3; TGF-β1, transforming growth factor-β1.

kidney of UUO mice. Except for EGFR, expressions of above indicators were reversed significantly by HDD treatment ($P < 0.05$, Figure 7A and B). In IHC staining, the expressions of PI3K, P-Stat3, and P-Src were significantly increased ($P < 0.001$), while MMP9 ($P < 0.001$) was markedly decreased in the kidney of UUO mice (Figure 7C and D). However, HDD treatment significantly reversed these alterations in UUO mice ($P < 0.001$). In vitro, HDD downregulated the expressions of α-SMA, P-EGFR, PI3K, and P-Stat3 induced by TGF-β1 in HK-2 cells (Figure 8A and B). Furthermore, EGFR agonist NSC228155 exacerbated TGF-β1-induced α-SMA expression but could be attenuated by combined treatment with HDD (Figure 8C and D). Similarly, HDD weakened the profibrotic effect of Stat3 agonist colivelin on TGF-β1-stimulated HK-2 cells (Figure 8E and F). These results revealed that HDD treatment was able to significantly regulate the expression of several targets that screened from NP in UUO mice kidney and TGF-β1-induced HK-2 cells.

Discussion

In this study, we screened 25 components in HDD extract by combining UHPLC-QE-MS analysis and HERB database. Then, we identified 6 core common targets (PI3K, Stat3, Src, EGFR, MMP9, and MMP2) of the screened 25 components and renal fibrosis by NP. Following this, HDD was confirmed to diminish renal fibrosis and regulate the expression of the above 6 core proteins in the UUO mice model. Since these 6 core proteins are signals of epithelial-mesenchymal transition (EMT) and extracellular matrix (ECM) production/degradation pathways, this could be a form of therapy for how HDD combats renal fibrosis (Figure 9). This is the first study to investigate the anti-renal fibrosis effects and

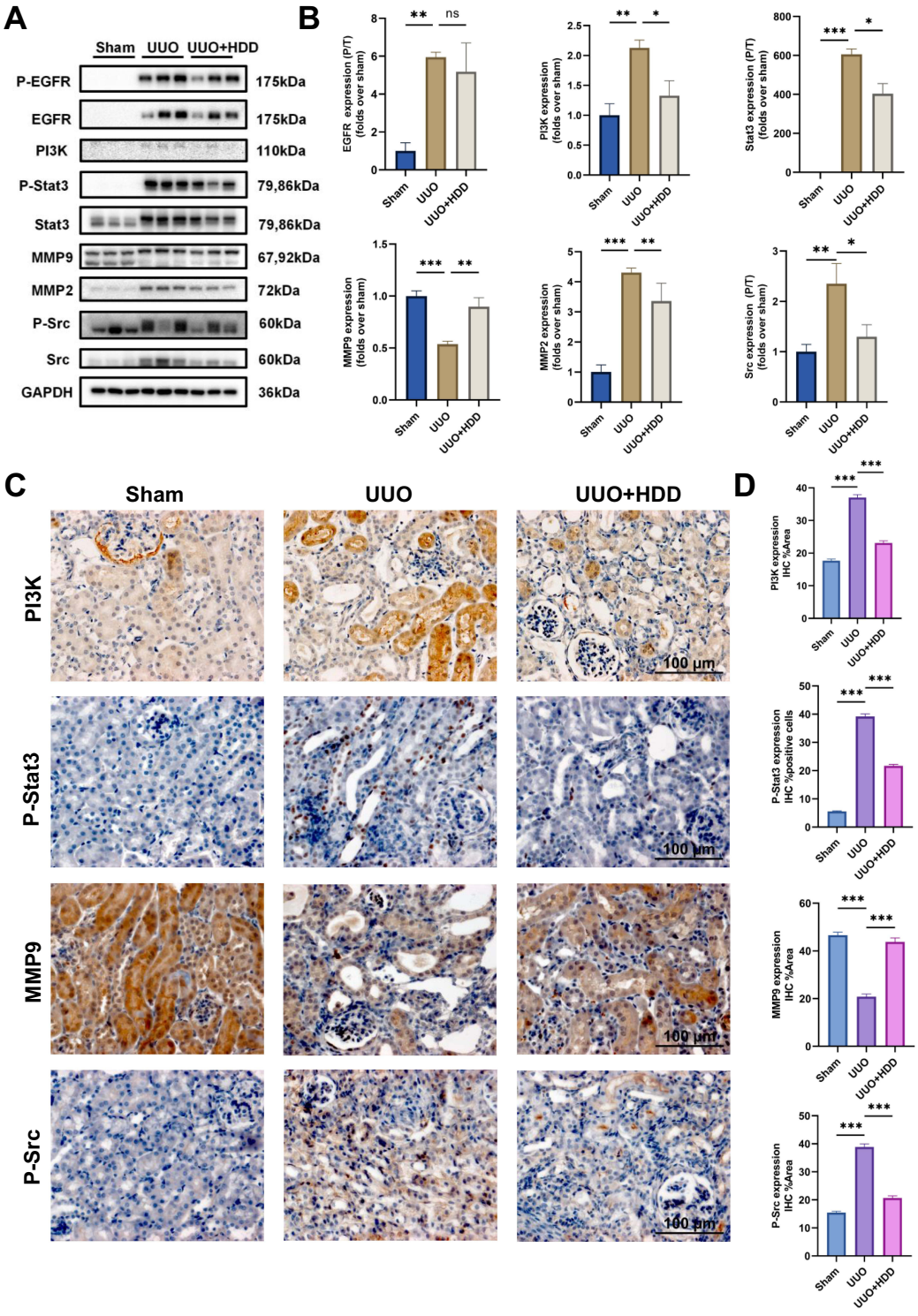

Figure 7 Effects of HDD on key targets expression in the kidneys of UUO mice. (**A**) Western blot images of P-EGFR, EGFR, PI3K, P-Stat3, Stat3, MMP9, MMP2, P-Src, and Src expression in kidney tissue. (**B**) Quantitative analysis of EGFR (phosphorylated/total), PI3K, Stat3 (phosphorylated/total), MMP9, MMP2, and Src (phosphorylated/total) expression, normalized to GAPDH. Data are expressed as the mean ± SEM, n = 6 mice per group, ns = no significance, **P* < 0.05, ***P* < 0.01, ****P* < 0.001. (**C**) Representative IHC images of PI3K, P-Stat3, MMP9, and P-Src. All images are shown at identical magnification, × 400, scale bar = 100 μm. (**D**) Quantitative analysis of PI3K, P-Stat3, MMP9, and P-Src expression in IHC. Data are expressed as the mean ± SEM, n = 5 mice per group, ****P* < 0.001.

Abbreviations: α-SMA, α-smooth muscle antibody; EGFR, epidermal growth factor receptor; GAPDH, glyceraldehyde-3-phosphate dehydrogenase; MMP2, matrix metalloproteinase-2; MMP9, matrix metalloproteinase-9; PI3K, phosphoinositide 3-kinase; Src, non-receptor tyrosine kinase Src; Stat3, signal transducer and activator of transcription 3; TGF-β1, transforming growth factor-β1.

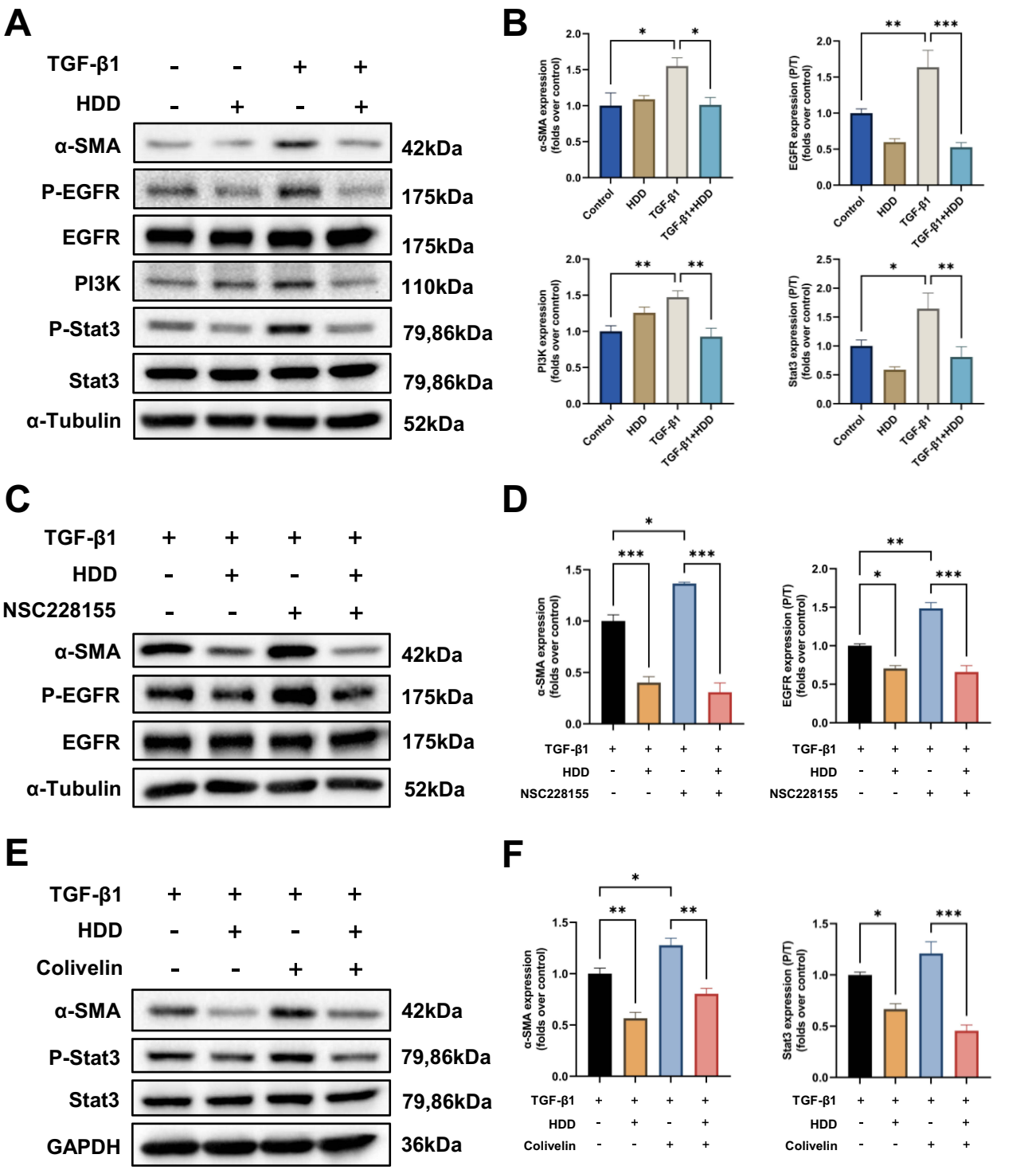

Figure 8 Effects of HDD on key targets expression in TGF-β1-induced HK-2 cells. (**A**) Western blot images of α-SMA, P-EGFR, EGFR, PI3K, P-Stat3, and Stat3 expression in HK-2 cells stimulated with TGF-β1 or/and HDD. (**B**) Quantitative analysis of α-SMA, EGFR (phosphorylated/total), PI3K, and Stat3 (phosphorylated/total) expression, normalized to α-Tubulin. (**C**) Western blot images of α-SMA, P-EGFR, and EGFR expression in TGF-β1-induced HK-2 cells treated with NSC228155 or/and HDD. (**D**) Quantitative analysis of α-SMA and EGFR (phosphorylated/total) expression, normalized to α-Tubulin. (**E**) Western blot images of α-SMA, P-Stat3, and Stat3 expression in TGF-β1-induced HK-2 cells treated with colivelin or/and HDD. (**F**) Quantitative analysis of α-SMA and Stat3 (phosphorylated/total) expression, normalized to GAPDH. Data are expressed as the mean ± SEM, n = 3–5 independent experiments, **P* < 0.05, ***P* < 0.01, ****P* < 0.001.

Abbreviations: α-SMA, α-smooth muscle antibody; EGFR, epidermal growth factor receptor; GAPDH, glyceraldehyde-3-phosphate dehydrogenase; PI3K, phosphoinositide 3-kinase; Stat3, signal transducer and activator of transcription 3; TGF-β1, transforming growth factor-β1.

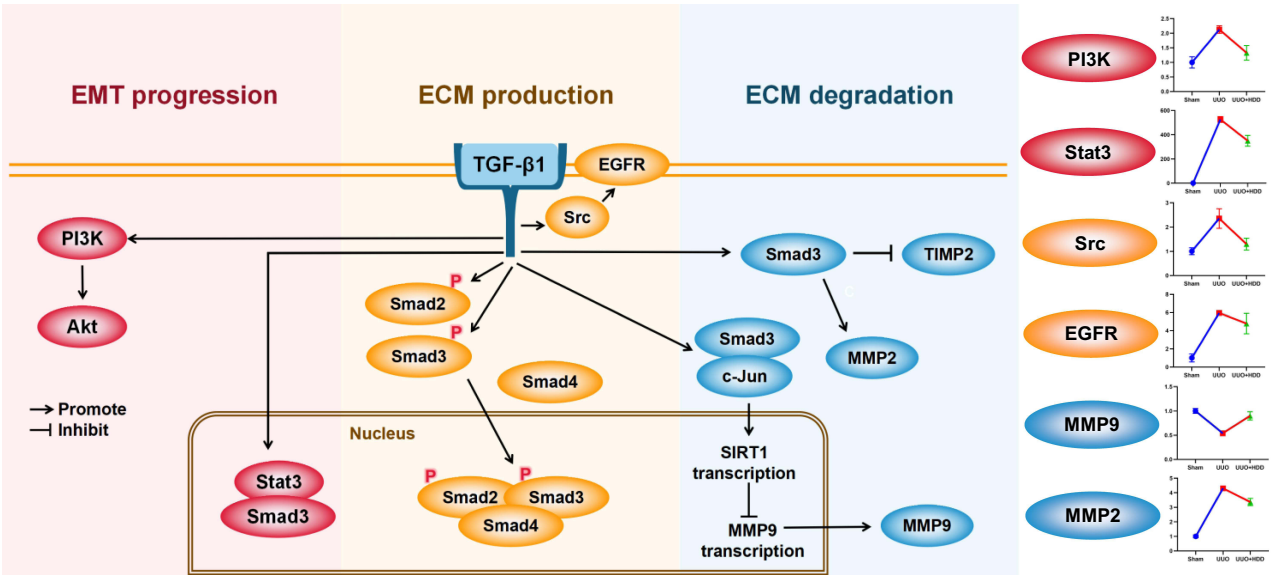

Figure 9 Schematic diagram showing potential mechanisms by which HDD antagonizes renal fibrosis.
Abbreviations: Akt, polyserine/threonine kinase; ECM, extracellular matrix; EGFR, epidermal growth factor receptor; EMT, epithelial-mesenchymal transition; MMP2, matrix metalloproteinase-2; MMP9, matrix metalloproteinase-9; PI3K, phosphoinositide 3-kinase; SIRT1, silent information regulator 1; Stat3, signal transduction and transcriptional activator 3; TGF-β1, transforming growth factor-β1; TIMP2, tissue inhibitors of metalloproteinase 2.

potential mechanisms of HDD in UUO mice model. The added value of this study lies in (1) providing evidence for the effectiveness of traditional Chinese medicine in treating renal fibrosis; and (2) providing a basis for screening compounds from HDD for treating renal fibrosis.

In CKD, fibrosis is the main pathological feature, and that severity is closely correlated with clinical prognosis.[4] In order to effectively treat CKD, renal fibrosis must be prevented and treated. ECM is produced and deposited in excess during the development of renal fibrosis, which results in the destruction of healthy kidney structures.[21] According to various studies, TGF-β1 affected ECM deposition in a variety of ways, leading to renal fibrosis.[22–24] Firstly, myofibroblasts are the primary cells responsible for producing ECM, and TGF-β1 can cause myofibroblast development by triggering the EMT process.[22] Secondly, TGF-β1 stimulates ECM production via a variety of signaling pathways that are either Smad-dependent or Smad-independent.[23] Thirdly, TGF-β1 suppresses matrix metalloproteinases (MMPs) and promotes tissue inhibitors of metalloproteinases (TIMP) to inhibit the degradation of ECM.[24] Using NP analysis in our study, it was found that 6 proteins including PI3K, Stat3, Src, EGFR, MMP9, and MMP2 were core common targets of HDD components and renal fibrosis. Further animal experiments validated that HDD could regulate the expression of these 6 proteins in the kidney of UUO mice. These 6 proteins are signals of EMT and ECM production/degradation pathways, suggesting that this could be a potential mechanism by which HDD antagonizes renal fibrosis. However, we did not use all pathway inhibitors or stimulators to confirm the specific signal pathways affected by HDD. This is a limitation of the present study. Further studies are needed to clarify the targets of HDD and screen effective small molecule compounds in HDD.

Regulation of EMT Progression

Several EMT responses brought on by TGF-β1 have been demonstrated to be mediated by the PI3K/Akt pathway.[25] TGF-β1 activation can either directly or indirectly activate the PI3K/Akt pathway. The PI3K/Akt pathway works with TGF-β1 for managing EMT in cancerous cells.[25–28] Additionally, pharmacological inhibitors of PI3K and Akt have been shown to block TGF-β1-induced EMT, cell migration, and osteoblast differentiation mediated by bone morphogenetic protein.[29] In our validation, we determined that the UUO model had a significantly greater TGF-β1 expression, and that HDD therapy had the opposite effect (Figure 6). Additionally, the expression of PI3K was decreased in the UUO+HDD group compared to the UUO group. These results are consistent with previous studies that PI3K is one of the key targets

which participate in controlling the progression of TGF-β1-induced EMT. In addition, HDD may reduce the expression of PI3K in order to reverse EMT progression. Additionally, Stat3 activation prevents interstitial fibroblasts in the UUO kidneys from being stimulated, which encourages renal fibrosis.[30] Stat3 activation can be induced by a variety of growth factors and cytokines such as TGF-β1. During tumorigenesis, Stat3 directly binds Smad3 and blocks its ability to form complexes with Smad4, thereby reducing the role TGF-β1 plays in promoting EMT.[31] Furthermore, by inactivating interstitial fibroblasts, the selective Stat3 inhibitor lowers obstructive nephropathy renal interstitial fibroblast activity and interstitial fibrosis.[32] In this research, it is found that P-Stat3 was expressed increasingly in UUO compared to Sham, indicating that Stat3 is closely related to the process of renal interstitial fibrosis (Figure 7C and D).

Stimulation of ECM Production

Among the most well-studied causes of fibrosis, TGF-β1 signaling induces myofibroblast activation through both Smad and non-Smad pathways.[33] TGF-β1 is a polymorphous cytokine that binds to its receptors on the cell membrane and activates Smad-dependent signaling. Smad2 and Smad3 become phosphorylated and connected to Smad4 to create Smad complexes. Matrix production is triggered by the Smad complex translocating into the nucleus.[34] In this study, the expressions of TGF-β1 and Smad2/3 were significantly greater in the UUO group than in the Sham group, whilst HDD treatment reversed the increase (Figure 6). These results indicated that HDD improved renal condition of UUO mice by modulating TGF-β1/Smad signaling pathway. Besides Smad dependent signaling pathway, TGF-β1 also promotes matrix production through non-Smad-dependent signaling pathways.[35] Recent research has demonstrated that TGF-β1 can quickly and briefly transactivate the EGFR and then trigger the production of FN without first activating Smad2. TGF-β1 can reactivate EGFR in rat mesangial cells via a Src kinase-mediated ligand-independent pathway.[34] TGF-β1 stimulates ECM upregulation through the Src/EGFR pathway.[36] In our research, we discovered that UUO had much higher levels of Src and EGFR expression than Sham, suggesting a key role for Src and EGFR in non-Smad-dependent signaling pathways. Additionally, HDD treatment tended to lessen the stimulation of the Src/EGFR signaling pathway.

Inhibition of ECM Degradation

A net accumulation of collagen in the tissue results in the formation of the extracellular matrix. This is due to an imbalance between collagen synthesis and degradation. Various MMPs and their inhibitors regulate both collagen transition and ECM degradation.[37] It has been proposed that the stimulation of the TGF-β1/Smad3 signaling pathway could trigger the transcription of SIRT1 along with c-Jun. By inhibiting the transcription of the MMP9 promoter, SIRT1 was able to fix MMP9 in the OFF mode. In contrast, the ON mode of MMP9 remained when Smad3 was lacking.[38] It was shown in Figure 7 that compared to the Sham, MMP9 expression was lower in UUO, and HDD treatment upregulated MMP9 expression in UUO mice. Moreover, activated MMP2 acts as a drill during the enzymatic hydrolysis of ECM components and is capable of rapidly binding fibrin. Mechanistically, the transcriptional activator Smad3 activates MMP2 and represses tissue inhibitors of metalloproteinases 2.[39] Thus, as shown in Figures 6 and 7, the over-expression of MMP2 may be due to up-regulation of Smad2/3 expression. Furthermore, in models of gastric cancer, the succinyl group of fibrillin 1 prevents MMP2 from adhering to it and prevents fibrillin 1 degradation.[40] This could also be an explanation for the increased MMP2 content. In agreement with other studies, our results suggest that HDD increases MMP9 and decreases MMP2 expression to improve ECM degradation and thus attenuate renal fibrosis.

Conclusion

Overall, through NP and experimental validation, our findings suggest that HDD may alleviate renal fibrosis by delaying EMT progression, reducing ECM production, and promoting ECM degradation. The construction of a critical target network for HDD mitigation of renal fibrosis may provide an experimental basis for clinical therapy of CKD. However, it still needs more research to determine the precise effects of the HDD components on the targets.

Abbreviations

BUN, blood urea nitrogen; CKD, chronic kidney disease; EGFR, epidermal growth factor receptor; EMT, epithelial-mesenchymal transition; FN, fibronectin; MMP2, matrix metalloproteinase-2; MMP9, matrix metalloproteinase-9;

MMPs, matrix metalloproteinases; PAS, periodic acid-Schiff; P-EGFR, Phospho-epidermal growth factor receptor; P-Smad2/3, Phospho-Smad2/3; P-Src, Phospho-Src; P-Stat3, Phospho-Stat3; SEM, standard error of mean; TIMP, tissue inhibitors of metalloproteinases; TGF-β1, transforming growth factor-β1; α-SMA, α-smooth muscle antibody.

Author Contributions

All authors made a significant contribution to the work reported, whether that is in the conception, study design, execution, acquisition of data, analysis and interpretation, or in all these areas; took part in drafting, revising or critically reviewing the article; gave final approval of the version to be published; have agreed on the journal to which the article has been submitted; and agree to be accountable for all aspects of the work.

Funding

Shenzhen Science and Technology Program [grant numbers JCYJ20210324111210029 and JCYJ20220531092214032] provided funding for this work.

Disclosure

The authors declare that they have no competing interests in this work.

References

1. Glassock RJ, Warnock DG, Delanaye P. The global burden of chronic kidney disease: estimates, variability and pitfalls. *Nat Rev Nephrol*. 2017;13(2):104–114. doi:10.1038/nrneph.2016.163
2. August P. Chronic Kidney Disease - Another Step Forward. *N Engl J Med*. 2023;388(2):179–180. doi:10.1056/NEJMe2215286
3. Webster AC, Nagler EV, Morton RL, Masson P. Chronic Kidney Disease. *Lancet*. 2017;389(10075):1238–1252. doi:10.1016/S0140-6736(16)32064-5
4. François H, Chatziantoniou C. Renal fibrosis: recent translational aspects. *Matrix Biol*. 2018;68-69:318–332. doi:10.1016/j.matbio.2017.12.013
5. Panizo S, Martínez-Arias L, Alonso-Montes C, et al. Fibrosis in Chronic Kidney Disease: pathogenesis and Consequences. *Int J Mol Sci*. 2021;22(1):408. doi:10.3390/ijms22010408
6. Zhang HW, Lin ZX, Xu C, Leung C, Chan LS. Astragalus (a traditional Chinese medicine) for treating chronic kidney disease. *Cochrane Database Syst Rev*. 2014;2014(10):Cd008369. doi:10.1002/14651858.CD008369.pub2
7. Pang H, Wu L, Tang Y, Zhou G, Qu C, Duan JA. Chemical Analysis of the Herbal Medicine Salviae miltiorrhizae Radix et Rhizoma (Danshen). *Molecules*. 2016;21(1):51. doi:10.3390/molecules21010051
8. Chen YC, Chen HT, Yeh CC, Hung SK, Yu BH. Four prescribed Chinese herbal medicines provide renoprotection and survival benefit without hyperkalemia risk in patients with advanced chronic kidney disease: a nationwide cohort study. *Phytomedicine*. 2022;95:153873. doi:10.1016/j.phymed.2021.153873
9. Su CY, Ming QL, Rahman K, Han T, Qin LP. Salvia miltiorrhiza: traditional medicinal uses, chemistry, and pharmacology. *Chin J Nat Med*. 2015;13(3):163–182. doi:10.1016/S1875-5364(15)30002-9
10. Huang X, Gao L, Deng R, et al. Huangqi-Danshen decoction reshapes renal glucose metabolism profiles that delays chronic kidney disease progression. *Biomed Pharmacother*. 2023;164:114989. doi:10.1016/j.biopha.2023.114989
11. Liu X, Huang S, Wang F, et al. Huangqi-Danshen Decoction Ameliorates Adenine-Induced Chronic Kidney Disease by Modulating Mitochondrial Dynamics. *Evid Based Complement Alternat Med*. 2019;2019:9574045. doi:10.1155/2019/9574045
12. Wei X, Wang Y, Weng J, et al. Combination of Perindopril Erbumine and Huangqi-Danshen Decoction Protects Against Chronic Kidney Disease via Sirtuin3/Mitochondrial Dynamics Pathway. *Evid Based Complement Alternat Med*. 2022;2022:5812105. doi:10.1155/2022/5812105
13. Liu X, Zhang B, Huang S, et al. Metabolomics Analysis Reveals the Protection Mechanism of Huangqi-Danshen Decoction on Adenine-Induced Chronic Kidney Disease in Rats. *Front Pharmacol*. 2019;10:992. doi:10.3389/fphar.2019.00992
14. Zhu X, Yao Q, Yang P, et al. Multi-omics approaches for in-depth understanding of therapeutic mechanism for Traditional Chinese Medicine. *Front Pharmacol*. 2022;13:1031051. doi:10.3389/fphar.2022.1031051
15. Nogales C, Mamdouh ZM, List M, Kiel C, Casas AI, Schmidt H. Network pharmacology: curing causal mechanisms instead of treating symptoms. *Trends Pharmacol Sci*. 2022;43(2):136–150. doi:10.1016/j.tips.2021.11.004
16. Li X, Liu Z, Liao J, Chen Q, Lu X, Fan X. Network pharmacology approaches for research of Traditional Chinese Medicines. *Chin J Nat Med*. 2023;21(5):323–332. doi:10.1016/S1875-5364(23)60429-7
17. Smith CA, Want EJ, O'Maille G, Abagyan R, Siuzdak G. XCMS: processing mass spectrometry data for metabolite profiling using nonlinear peak alignment, matching, and identification. *Anal Chem*. 2006;78(3):779–787. doi:10.1021/ac051437y
18. Fang S, Dong L, Liu L, et al. HERB: a high-throughput experiment- and reference-guided database of traditional Chinese medicine. *Nucleic Acids Res*. 2021;49(D1):D1197–d1206. doi:10.1093/nar/gkaa1063
19. Chevalier RL, Forbes MS, Thornhill BA. Ureteral obstruction as a model of renal interstitial fibrosis and obstructive nephropathy. *Kidney Int*. 2009;75(11):1145–1152. doi:10.1038/ki.2009.86
20. Cortes AL, Gonsalez SR, Rioja LS, et al. Protective outcomes of low-dose doxycycline on renal function of Wistar rats subjected to acute ischemia/reperfusion injury. *Biochim Biophys Acta Mol Basis Dis*. 2018;1864(1):102–114. doi:10.1016/j.bbadis.2017.10.005
21. Zhang Y, Li K, Li Y, et al. Profibrotic mechanisms of DPP8 and DPP9 highly expressed in the proximal renal tubule epithelial cells. *Pharmacol Res*. 2021;169:105630. doi:10.1016/j.phrs.2021.105630

22. Li YK, Ma DX, Wang ZM, et al. The glucagon-like peptide-1 (GLP-1) analog liraglutide attenuates renal fibrosis. *Pharmacol Res*. 2018;131:102–111. doi:10.1016/j.phrs.2018.03.004
23. Lan HY, Chung AC. TGF-β/Smad signaling in kidney disease. *Semin Nephrol*. 2012;32(3):236–243. doi:10.1016/j.semnephrol.2012.04.002
24. Border WA, Noble NA. Evidence that TGF-beta should be a therapeutic target in diabetic nephropathy. *Kidney Int*. 1998;54(4):1390–1391. doi:10.1046/j.1523-1755.1998.00127.x
25. Asano Y, Ihn H, Yamane K, Jinnin M, Mimura Y, Tamaki K. Phosphatidylinositol 3-kinase is involved in alpha2(I) collagen gene expression in normal and scleroderma fibroblasts. *J Immunol*. 2004;172(11):7123–7135. doi:10.4049/jimmunol.172.11.7123
26. Luo K. Signaling Cross Talk between TGF-β/Smad and Other Signaling Pathways. *Cold Spring Harb Perspect Biol*. 2017;9(1):a022137. doi:10.1101/cshperspect.a022137
27. Jeong HW, Kim IS. TGF-beta1 enhances betaig-h3-mediated keratinocyte cell migration through the alpha3beta1 integrin and PI3K. *J Cell Biochem*. 2004;92(4):770–780. doi:10.1002/jcb.20110
28. Lechuga CG, Hernández-Nazara ZH, Domínguez Rosales JA, et al. TGF-beta1 modulates matrix metalloproteinase-13 expression in hepatic stellate cells by complex mechanisms involving p38MAPK, PI3-kinase, AKT, and p70S6k. *Am J Physiol Gastrointest Liver Physiol*. 2004;287(5):G974–987. doi:10.1152/ajpgi.00264.2003
29. Ghosh-Choudhury N, Abboud SL, Nishimura R, Celeste A, Mahimainathan L, Choudhury GG. Requirement of BMP-2-induced phosphatidylinositol 3-kinase and Akt serine/threonine kinase in osteoblast differentiation and Smad-dependent BMP-2 gene transcription. *J Biol Chem*. 2002;277(36):33361–33368. doi:10.1074/jbc.M205053200
30. Kuratsune M, Masaki T, Hirai T, et al. Signal transducer and activator of transcription 3 involvement in the development of renal interstitial fibrosis after unilateral ureteral obstruction. *Nephrology*. 2007;12(6):565–571. doi:10.1111/j.1440-1797.2007.00881.x
31. Wang G, Yu Y, Sun C, et al. STAT3 selectively interacts with Smad3 to antagonize TGF-β signalling. *Oncogene*. 2016;35(33):4388–4398. doi:10.1038/onc.2015.446
32. Pang M, Ma L, Gong R, et al. A novel STAT3 inhibitor, S3I-201, attenuates renal interstitial fibroblast activation and interstitial fibrosis in obstructive nephropathy. *Kidney Int*. 2010;78(3):257–268. doi:10.1038/ki.2010.154
33. Park JH, Jang KM, An HJ, et al. Pomolic Acid Ameliorates Fibroblast Activation and Renal Interstitial Fibrosis through Inhibition of SMAD-STAT Signaling Pathways. *Molecules*. 2018;23(9):2236. doi:10.3390/molecules23092236
34. Chen Y, Peng FF, Jin J, Chen HM, Yu H, Zhang BF. Src-mediated ligand release-independent EGFR transactivation involves TGF-β-induced Smad3 activation in mesangial cells. *Biochem Biophys Res Commun*. 2017;493(2):914–920. doi:10.1016/j.bbrc.2017.09.121
35. Meng XM, Nikolic-Paterson DJ, Lan HY. TGF-β: the master regulator of fibrosis. *Nat Rev Nephrol*. 2016;12(6):325–338. doi:10.1038/nrneph.2016.48
36. Yi JY, Shin I, Arteaga CL. Type I transforming growth factor beta receptor binds to and activates phosphatidylinositol 3-kinase. *J Biol Chem*. 2005;280(11):10870–10876. doi:10.1074/jbc.M413223200
37. Verrecchia F, Mauviel A. TGF-beta and TNF-alpha: antagonistic cytokines controlling type I collagen gene expression. *Cell Signal*. 2004;16(8):873–880. doi:10.1016/j.cellsig.2004.02.007
38. Warburton D, Shi W, Xu B. TGF-β-Smad3 signaling in emphysema and pulmonary fibrosis: an epigenetic aberration of normal development? *Am J Physiol Lung Cell Mol Physiol*. 2013;304(2):L83–85. doi:10.1152/ajplung.00258.2012
39. Lian GY, Wang QM, Mak TS, Huang XR, Yu XQ, Lan HY. Inhibition of tumor invasion and metastasis by targeting TGF-β-Smad-MMP2 pathway with Asiatic acid and Naringenin. *Mol Ther Oncolytics*. 2021;20:277–289. doi:10.1016/j.omto.2021.01.006
40. Wang X, Shi X, Lu H, et al. Succinylation Inhibits the Enzymatic Hydrolysis of the Extracellular Matrix Protein Fibrillin 1 and Promotes Gastric Cancer Progression. *Adv Sci*. 2022;9(27):e2200546. doi:10.1002/advs.202200546